



**Antioxidant-Induced Transformations of a Metal-Acid
Hydrocracking Catalyst in the Deconstruction of
Polyethylene Waste**

Journal:	<i>Green Chemistry</i>
Manuscript ID	GC-COM-07-2022-002503.R1
Article Type:	Communication
Date Submitted by the Author:	04-Aug-2022
Complete List of Authors:	<p>Hinton, Zachary; University of Delaware, Center for Plastics Innovation Kots, Pavel; University of Delaware, Center for Plastics Innovation Soukaseum, Mya; University of Delaware, Center for Plastics Innovation; University of Delaware, Department of Chemical and Biomolecular Engineering Vance, Brandon; University of Delaware, Center for Plastics Innovation; University of Delaware, Department of Chemical and Biomolecular Engineering Vlachos, Dionisios; University of Delaware, Center for Plastics Innovation; University of Delaware, Department of Chemical and Biomolecular Engineering Epps, III, Thomas; University of Delaware, Center for Plastics Innovation; University of Delaware, Department of Chemical and Biomolecular Engineering; University of Delaware, Department of Materials Science and Engineering Korley, LaShanda; University of Delaware, Center for Plastics Innovation; University of Delaware, Department of Chemical and Biomolecular Engineering; University of Delaware, Department of Materials Science and Engineering</p>

Antioxidant-Induced Transformations of a Metal-Acid Hydrocracking Catalyst in the Deconstruction of Polyethylene Waste

Zachary R. Hinton^{1,*}, Pavel A. Kots^{1,*}, Mya Soukaseum^{1,2}, Brandon C. Vance^{1,2}, Dionisios G. Vlachos^{1,2}, Thomas H. Epps, III^{1,2,3,†}, LaShanda T. J. Korley^{1,2,3,†}

¹Center for Plastics Innovation, University of Delaware, Newark, DE 19716

²Department of Chemical and Biomolecular Engineering, University of Delaware, Newark, DE 19716

³Department of Materials Science and Engineering, University of Delaware, Newark, DE 19716

*These authors contributed equally

†Corresponding authors

Abstract

Plastics are ideal for numerous applications, as driven by the development of complex formulations containing various additives to improve performance and processability. Unfortunately, chemical valorization strategies (e.g., catalytic deconstruction) often can be challenged by the presence of small-molecule additives, and quantification of the impact of these molecular constituents on upcycling processes remains elusive. This dearth of information restricts catalyst design efforts to combine the robustness and performance necessary to improve plastics circularity. In this communication, we describe a systematic study of a common plastics additive—phenolic antioxidants, and we quantify the relationship between additive content and deconstruction yields of high-density polyethylene (HDPE) over a platinum on tungstated zirconium ($\text{Pt}/\text{WO}_3/\text{ZrO}_2$) hydrocracking catalyst. In the simplest case of a base (antioxidant- and slip agent-containing) HDPE resin versus a pure (additive-stripped) HDPE polymer, a two-fold decrease in the yield of gas and liquid products is noted for base HDPE resin. Furthermore, both antioxidant chemistry and concentration strongly impact conversion and individual product selectivities. Using infrared spectroscopy, we determine that antioxidants change the effective ratio of metal to acid sites (i.e., metal-acid balance) through reactions of phenols and/or other functional groups (e.g., acids, esters) with catalyst active sites. Overall, this work demonstrates the impact of one common set of additives on plastics deconstruction, and the analysis herein provides a blueprint for quantitatively assessing the effects of additives on plastics deconstruction processes and for evaluating the development of more robust catalytic strategies or more tolerable additive formulations.

Introduction

The increased global consumption of plastics is a direct result of the numerous benefits of polymers (e.g., barrier properties, high strength-to-weight ratio).^{1, 2} This accelerating demand for plastics is accompanied by manufacturer and consumer needs for an amalgam of features (e.g., visual appeal, thermal stability, versatile processability) that drive rising plastics diversity. Polymer types, chemical additives, inorganic co-materials (e.g., metal, paper), form factors, advanced processing and thermal histories, etc. contribute to highly varied waste streams that challenge the creation of economic value and reduction of waste accumulation.^{1, 3, 4} For example, within

sorted, post-consumer high-density polyethylene (HDPE), numerous colorants, processing aids, macromolecular architectures, fillers, and crystallinities can be present and can introduce significant heterogeneity among recycling inputs (to either mechanical or chemical processes) that limits product value and process scalability.⁴⁻⁶ Valorization routes that consider both the macromolecular and the compositional diversity inherent to all plastics are likely to become widespread strategies that address real, discarded plastics.^{3, 4, 7}

Plastics waste contains a vast array of small-molecule additives.^{8, 9} Many commercial polymers require additives to facilitate processability and improve performance.^{6, 10, 11} For example, HDPE can often contain processing aids that enable molding or extrusion, and certain applications (e.g., outdoor furniture, electronics packaging) necessitate the inclusion of additives, such as ultraviolet (UV) stabilizers or antistatic agents.^{9, 10} Similar formulation considerations are made for most commodity polymers.⁹ Although 25 Mt of plastics additives were produced globally in 2015 (equivalent to the production of polystyrene),² only a small fraction of the over 10,000 individual chemical substances have been widely studied with respect to their direct impact on chemical deconstruction of polymers.⁸ Yet, it has been widely speculated that both mechanical and chemical re/upcycling processes are significantly impacted by additives.^{6, 8, 12, 13}

Experimental studies of valorization processes that treat specific plastic products (e.g., packaging, cables) highlight the challenges posed by additives.⁶ For example, brominated flame retardants in electronics waste diminish deconstruction activity by poisoning catalysts and contribute to lower product stream purity and value.¹⁴ In another instance, dissolution- or solvolysis-based approaches can concentrate certain toxic additives like phthalate plasticizers, precluding industrial adoption.^{7, 15} Although the impact of additives on valorization is widely accepted as fact or implied by experimental studies,^{1, 16-18} information about how common additives affect certain emergent chemical recycling strategies is needed to guide innovation in both plastics formulation and catalytic design. As scientific advances continue to address increasingly complex waste, novel processes that are tolerant to a wide range of additives are highly desirable.^{1, 4, 19}

Hydroconversion (*i.e.*, hydrocracking and hydrogenolysis) has gained increasing attention as a strategy for the deconstruction of plastics.^{1, 18, 20-22} This technology is particularly well suited to valorize polyolefins, which represent the largest percentage (by weight) of plastics consumed globally.² In hydroconversion processes, supported noble metal catalysts (e.g., platinum on tungstated zirconia, ruthenium on titanium dioxide) or solid acids (e.g., zeolites, tungstated zirconia) facilitate increased bond-scission activity and value-added product selectivity at mild operating conditions and short reaction times.^{1, 18, 20-22} For example, our previously developed bifunctional hydrocracking catalyst, platinum on tungstated zirconium (Pt/WO₃/ZrO₂), exhibits high activity for polyolefin hydrocracking to alkane products. Furthermore, the selectivity of this catalyst toward desired molecular weights or degrees of branching can be easily controlled by alteration of the metal-acid balance [MAB, *i.e.*, the molar ratio of Pt sites to Brønsted acid (BA) sites].^{20, 21} Unfortunately, the highly tunable nature of many hydroconversion catalysts is often countered by susceptibility to poisoning,^{18, 23, 24} and this vulnerability is particularly important when considering hydroconversion approaches to treat real plastics waste.

In this work, we quantify the activity of our model catalyst, Pt/WO₃/ZrO₂, as impacted by common plastic additives. We examine the deconstruction of as-received HDPE (*i.e.*, base resin) to demonstrate the high activity of Pt/WO₃/ZrO₂. We then identify the small-molecule additives present in the base resin and reveal the effect that typical additives have on product yield and distribution by deconstructing pure (*i.e.*, stripped of additives) HDPE polymer. Next, we focus on the role of specific phenolic antioxidants in the reduction of activity and in the alteration of product distribution by adding three common molecules to HDPE. Our results indicate that both additive

concentration and chemical structure contribute to changes to the effective MAB of Pt/WO₃/ZrO₂, and consequently, effect differences in product distributions. Finally, spectroscopic analysis is used to probe the chemical nature of the catalyst before and after poisoning by antioxidants. Our results reveal that the phenolic group of these small-molecule additives can generate phenoxy species that consume catalyst active sites; however, more severe poisoning can be caused by antioxidants that contain additional functional groups (e.g., acids, esters). These findings suggest that selection of antioxidants (and other additives) for plastic formulations with higher valorization potential should consider the potential effects of both additive loading and chemical structure.

Results and discussion

Initially, we quantified hydrocracking performance for as-received HDPE pellets (weight-average molecular weight, M_w , ~ 90 kg/mol, melt flow index = 12 g / 10 min, purchased from Sigma Aldrich), which contained a basic additive profile that facilitates processing during the fabrication of plastic products.^{6, 9, 10} For all experiments, the catalyst to polymer mass ratio was fixed at 1:40 so that sufficient masses (typically > 200 mg) of solid residues remained to be analyzed. This value was selected based on preliminary experiments, the results of which are given in **Figures S1-S3** and discussed in the **Supporting Information (SI)**. The detailed synthetic protocol and characterization of the catalyst are reported elsewhere.²¹ The overall activity measured in this study is higher than previously reported for LDPE at otherwise identical experimental conditions.²¹ The results in **Figure 1a** show that Pt/WO₃/ZrO₂ cracked HDPE to extractable (*i.e.*, gas and liquid) products with moderate yield (20%, on a moles of carbon basis as described in the **SI**). The product distributions obtained from gas chromatography with flame ionization detection (GC-FID) for the extractables (**Figure 1b**) and high-temperature gel permeation chromatography (HT-GPC) for the solids (**Figure 1c**) indicated the most abundant products, C₇₋₁₀ and C_{~30}, were accompanied by a significant amount of unreacted HDPE.

To examine the effect of the native additives on hydrocracking performance, we compared the base HDPE resin results with those for a stripped HDPE. This purified polymer was recrystallized (by slowly cooling a 6 wt% solution in toluene from 130 °C) and extracted (*via* 24 h Soxhlet extraction in chloroform) such that the majority of additives were removed. A clear increase in activity was measured for the stripped HDPE sample, whereby extractable (*i.e.*, gas and liquid) yield was enhanced from 20% (pellets) to 86% (stripped) (**Figure 1a**). It is important to note that our extraction procedure resulted in HDPE particle diameters of ~30 μm (*i.e.*, a powder), whereas the original pellets were ~4 mm. A more uniform distribution of the catalyst within the HDPE melt at the start of the reaction was achieved for the powder form, in comparison to the pellets, and likely was a key factor in the increase in measured catalyst activity (**Figure S4**). Therefore, stripped HDPE is more appropriately compared to a powdered HDPE, which for this study had the same particle size, because it was formed by recrystallization, but retained the additives in the as-received HDPE, as it was dried from solution without extraction. It should be noted that there is the potential for degradation of additives (particularly antioxidants) during the stripping process; however, it is likely that this reaction does not reduce the concentration of antioxidants significantly enough to affect our results. This powdered HDPE led to higher activity (44% extractables yield) than pellets (20%); however, the effect of additives remained pronounced with respect to the stripped HDPE (**Figure 1a**).

Comparison of the product streams from the powdered and stripped HDPE samples suggests that the effect of the base additive profile leads to a dramatic change in the overall kinetics (or activity). The yields of individual components of the extractable products are shown in **Figure 1b**. Although the distributions were similar, the ratio of selectivities toward carbon number 5 and 10

products was nearly double for the stripped HDPE (0.9) in comparison to both the pellet and powdered HDPE (0.48). This shift toward lower-molecular-weight alkanes suggested secondary cracking of the alkane products. The solid product distributions (**Figure 1c**) demonstrated a similar trend. One key effect of additive removal was to increase the production of heavy (solid) alkanes, likely because of the occurrence of deeper cracking of intermediate waxes, and this cause is distinct from a change in conversion (e.g., from different catalyst loadings, see **SI**). Although hydrogen has been proposed to mitigate the impact of impurities on deconstruction,¹⁵ the results herein indicate that even base additive formulations can lower deconstruction reaction rates. Furthermore, mass transfer effects are likely important for both the polymer and small-molecule additives and are the subject of ongoing work.

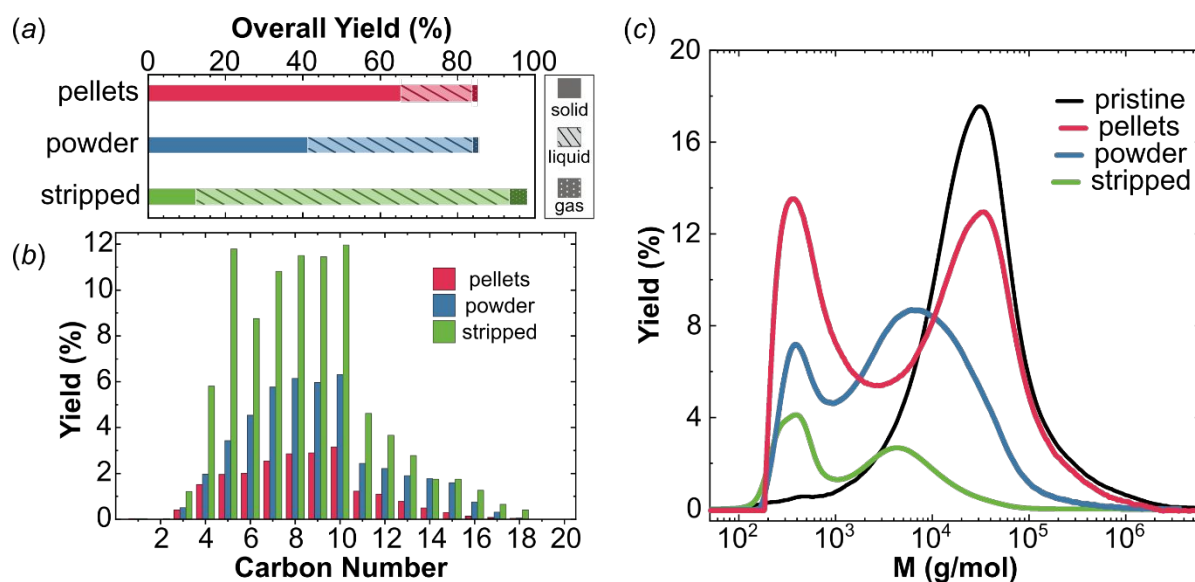


Figure 1. Deconstruction product analysis for various forms of HDPE: as-received pellets, powdered (retaining additives), and stripped of additives. (a) Overall yield of solid, liquid, and gas products, (b) extractable yields as a function of carbon number, and (c) solid product yields as a function of molecular weight. The molecular weight distribution of pristine HDPE pellets is included in (c) and was arbitrarily shifted to an overall solid yield of 50%. Pristine distributions for powdered and stripped HDPE are given in Figure S8. Reaction conditions: 250 °C, 30 bar H₂, 2 g HDPE, 50 mg Pt/WO₃/ZrO₂, 2 h.

To further examine the effects of base HDPE formulation on catalytic activity, we catalogued the specific additive chemistries extracted from our stripped HDPE. Four small-molecule additives were identified by gas chromatography-mass spectrometry (GC-MS): two primary, hindered-phenolic antioxidants and two fatty-amide slip agents (**Figures S5-S8** and **Table S1**). It should be noted that larger-molecular-weight additives (*i.e.*, phenolic phosphite secondary antioxidants) likely were present,¹⁰ but they could not be detected by GC-MS. Importantly, the inputs to most previously reported polyethylene-deconstruction processes have unwittingly contained additives from a (typically uncharacterized) base formulation that may be similar in composition to the HDPE in this work. Thus, many of these studies have drawn conclusions about polymer- or catalyst-specific effects but may be measuring the impact of additives to a substantial degree, and there exists a need to identify specific catalyst-additive interactions for common additives and catalyst. Given that most commercial plastics contain phenolic antioxidants,^{9, 10} fundamental

quantification of the impact of these molecules is useful for assessing the performance of additive-tolerant valorization strategies.

Towards such an evaluation, we investigated three phenolic antioxidants (of different molecular sizes and that contain different functional groups) at two concentrations (0.5 wt% and 2 wt%) to mimic typical formulation conditions^{10, 25, 26} and to emphasize the measured effects, respectively. The chemical structures of the antioxidants investigated in this work and overall product yields are summarized in **Figure 2**. Note that we did not select the antioxidants found in the original HDPE for further study in order to extend our results to a wider range of potential plastics formulations.¹⁰ Hydrocracking was performed using the same method as above with a fixed 1:40 mass ratio of catalyst to polymer to confine the reaction to the low-conversion regime. The measured overall yield of extractable products varied strongly as a function of the antioxidant chemistry and concentration (**Figure 2b**). In the absence of additives, the stripped HDPE was converted into mostly liquid products (81% yield); however, the HDPE samples that contained antioxidants always achieved less than 60% liquid yield. Less than 5% yield of gas was measured in all cases. With each different antioxidant chemistry, three distinct features were noted. For butylated hydroxytoluene (BHT), solid and liquid yields were comparable between the 0.5 wt% (43% and 40%) and 2 wt% (38% and 37%) loadings. This finding is a potential indicator of reversible poisoning (*i.e.*, an equal, equilibrium concentration of BHT was adsorbed on the catalyst). For Irganox[®] 1010 (I-1010), deconstruction inhibition was dependent on antioxidant concentration. At 0.5 wt% I-1010, the highest yield of liquid products of all antioxidant-containing samples was measured (58%), but, at 2 wt% I-1010, the liquid yield decreased significantly to 9%. For Irganox[®] 3114 (I-3114), < 2% extractable yield was achieved for both concentrations, which indicated severe, irreversible poisoning of the catalyst even at low concentration. These results suggest that antioxidants are a significant factor impacting catalytic activity of the base HDPE (**Figure 1**) and that specialty antioxidants (*e.g.*, I-3114) also poison hydrocracking catalysts.

The mechanism by which antioxidants interfere with hydrocracking was more complex than that measured for the base formulation of HDPE, as detailed by an analysis of product distributions obtained from GC-FID and HT-GPC analyses (**Figures 3, S9**). The discrete carbon numbers of alkanes in the gaseous and liquid products were converted to approximate molecular weights, and the overall yields were combined with the continuous distribution (in terms of yield) of the solid products. The resultant summed distributions were calculated and plotted as a function of the molecular weight (see calculation details in the **SI**). Clear differences in the shape of measured distributions arose due to the production of distinct alkane/polyethylene populations that generated overlapping signals. The distributions were divided into six product groups on the basis of approximate bounds that correspond to light fuels (C₁-C₈), alkanes (C₈-C₁₃), diesel fuels (C₁₃-C₂₃), fuel and lubricant oil (C₂₃-C₇₀), heavy wax/low molecular weight polymer (C₇₀-C₇₀₀), and pristine polymer (**Table S2**). A summary of the selectivities of these groups is given in **Figures 3c, 3d, S10**.

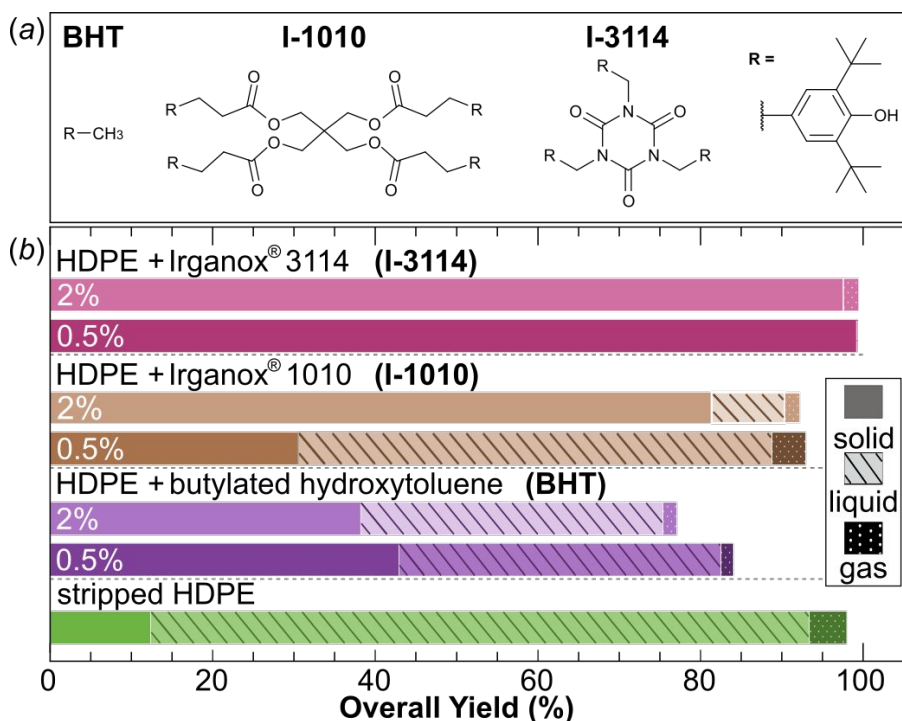


Figure 2. (a) The chemical structures of the antioxidants used in this work. (b) Overall yield of solid, liquid, and gas products for all antioxidant-containing HDPE samples (at 0.5 and 2 wt%) and HDPE stripped of additives. Labels indicate common trade names (Irganox[®] is a registered trademark of BASF group) and abbreviations. Reaction conditions: 250 °C, 30 bar H₂, 2 g HDPE, 50 mg Pt/WO₃/ZrO₂, 2 h.

For stripped HDPE, groups I, II, IV, and V were the most prominent products, with high conversion indicated by significant group I and II yields (**Figures 3a, 3c, S11**). For 0.5 wt% BHT, the product distribution was shifted to higher molecular weight products (*i.e.*, lower group I and II yields and higher amounts of unreacted polymer) due to lower activity. At 2 wt%, BHT led to similar product yields as 0.5 wt% except for group V products, which were diminished. A similar trend in selectivity was measured for the concentration dependence of I-1010 samples (**Figure 3b, 3d, S10**); however, at 2 wt% I-1010, conversion to groups I and II was eliminated in favor of group III, which indicated the catalyst was more severely poisoned at higher antioxidant levels. For I-3114, product distributions (**Figure S12**) showed only marginal yield of group III products in the solid fraction, which could be products generated at the early stages of the reaction before the antioxidant poisoned catalyst active sites. This result indicated that antioxidants reduce catalytic activity as cracking occurs, such that the conversion of waxy intermediates to small alkanes does not occur.

Comparison of the overall yield and composition of the solid residues further demonstrated the impact of antioxidant concentration and chemistry dependence on hydrocracking outcomes. A simple subtraction of a weighted pristine HDPE distribution from the measured product distribution (see details in the **SI**) was used to quantify unreacted HDPE in the solid products and to calculate a corrected selectivity of solid intermediates. This analysis demonstrated that overall solid yield is an insufficient indicator of conversion. Rather, quantification of the unreacted HDPE for antioxidant-containing samples (**Figure S13**) and different catalyst loadings (**Figure S14**) revealed that similar solid yields did not indicate the same conversion of HDPE. For example, as-received HDPE pellets, HDPE powder, and HDPE that contained 2 wt% BHT all yielded ~40%

solids (deconstructed at the same catalyst loading), but these residues contained ~35%, ~70%, and ~30% unreacted polymer, respectively (see **Figures S13-S14**). Although pristine Pt/WO₃/ZrO₂ led to a maximum yield of waxes (i.e., solid products) at 25%, in the presence of antioxidant, up to 40% yield of wax was achievable. A similar effect was measured in our previous study of LDPE deconstruction, wherein a series of Pt/WO₃/ZrO₂ catalysts of varied MAB produced similar solid yields but distinct molecular weight distributions for both the solid and extractable products.²¹ Therefore, the origin of the different product species distributions (**Figure 3**) was likely related to a dynamic MAB induced by poisoning of catalyst active sites.

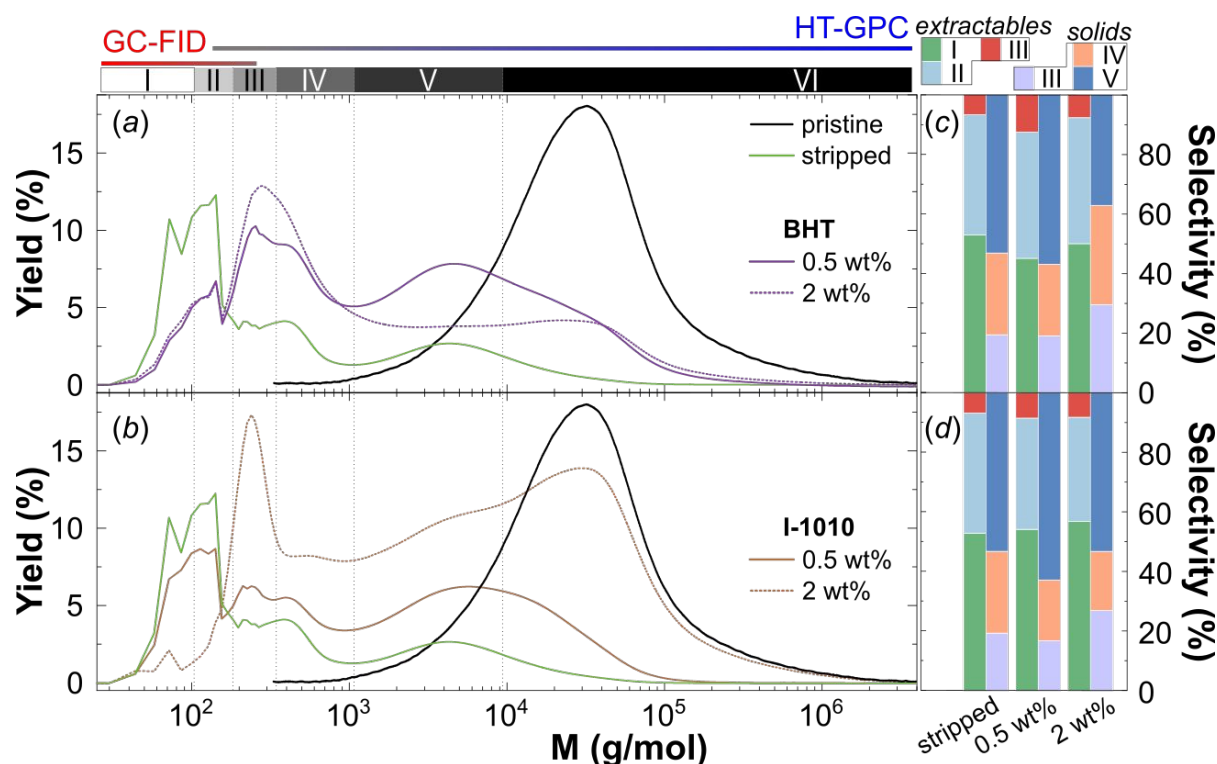


Figure 3. Product yield distribution for BHT- (a) and I-1010- (b) containing HDPE, which include distributions for pristine (arbitrarily shifted to a solid yield of 50%) and stripped HDPE. Ranges highlight approximate populations discussed in the text. Data for $M < 400$ g/mol are sums of the yields of extractable products (obtained from GC-FID) and solid products (obtained from HT-GPC) for approximately the same molecular weight. Typical ranges for M measured by both techniques are illustrated. Results for I-3114-containing HDPE are reported in **Figure S12**. Product selectivities of BHT (c) and I-1010 (d) for extractable and solid fractions. Solid selectivities were corrected for unreacted polymer. Reaction conditions: 250 °C, 30 bar H₂, 2 g HDPE, 50 mg Pt/WO₃/ZrO₂, 2 h.

To validate the dynamic MAB hypothesis and determine the cause of chemistry-specific antioxidant effects, catalyst particles were impregnated with solutions of antioxidants to facilitate adsorption/poisoning and then heated under hydrogen flow at 250 °C to simulate hydrocracking conditions. Two spectroscopic probe molecules were used to quantify antioxidant-catalyst interactions via diffuse reflectance infrared Fourier transform spectroscopy (DRIFTS): CO for Pt metal sites and pyridine for BA sites. The measured DRIFTS traces for pristine and poisoned catalyst exhibited antioxidant-mediated changes to the effective MAB. The metal sites of the pristine catalyst showed a strong carbonyl band at 2085 cm⁻¹ due to 8 to 9-fold coordinated Pt and a peak at 1855 cm⁻¹ caused by multiple sites bridged by CO (**Figure 4a**).²⁷ After treatment

with BHT and I-3114, well-coordinated Pt sites were eliminated, and a new band appeared at 2048 cm^{-1} , which indicated CO is bound to 6 to 7-fold (under) coordinated Pt sites.²⁷ Also, the band at 1855 cm^{-1} completely disappeared, which suggested that Pt flat facets were blocked by adsorbed antioxidant, but corner and edge sites with lower coordination number were unaffected. Semi-quantitative analysis of DRIFTS data indicated that 30-35% of Pt sites remain accessible to CO. Strong attractions between π -electrons in the aromatic ring of phenol and metal atoms on the flat surface have been previously reported²⁸ and were likely responsible for blocking Pt sites.

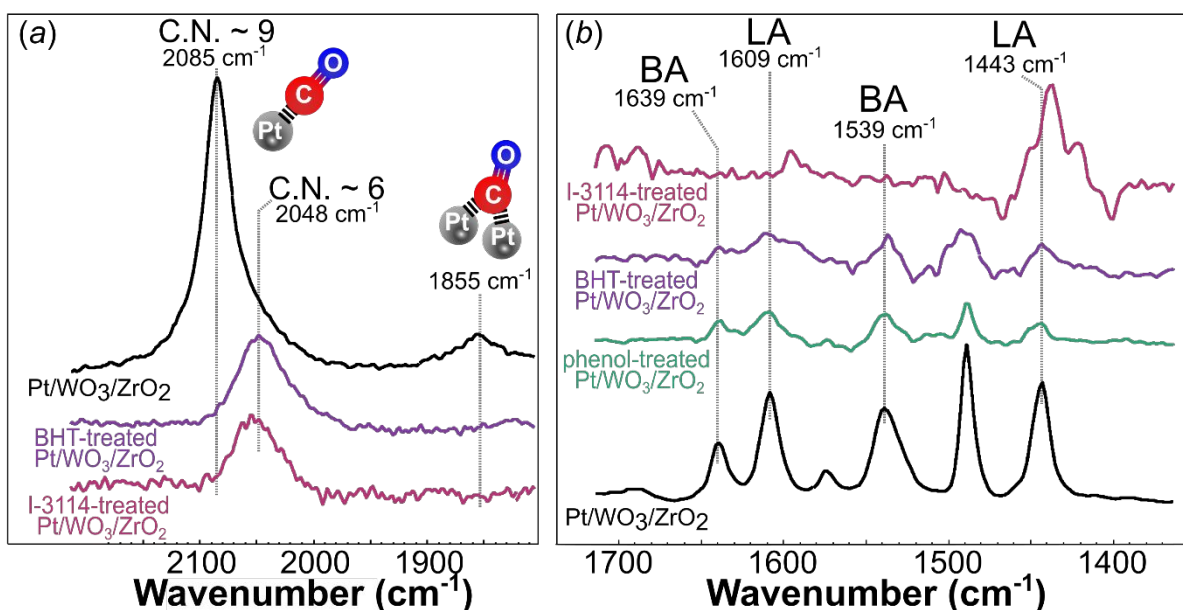


Figure 4. DRIFTS data for pure and antioxidant treated $\text{Pt}/\text{WO}_3/\text{ZrO}_2$ catalysts. (a) CO adsorption at 35 °C that highlights the region of linear and bridging carbonyls in which a reduction of coordination number (C.N.) is measured. (b) Pyridine chemisorption on acid sites at 150 °C that shows changes to relative concentration of Lewis acid (LA) and BA. Sample preparation conditions: solution deposition of molecules followed by drying and treatment at 250 °C under 10% H_2 in He flow for 2 h.

The bi-functional nature of our hydrocracking catalyst is key to activity, which makes selectivity and conversion dependent on both metal and acid sites.²¹ Quantification of antioxidant-mediated changes to BA sites via pyridine chemisorption on $\text{Pt}/\text{WO}_3/\text{ZrO}_2$ showed formation of protonated pyridine (characteristic bands at 1639 and 1539 cm^{-1}) bound to BA sites and pyridine coordinated to Zr^{4+} LA sites (bands at 1609 and 1443 cm^{-1}) (**Figure 4b**).²⁹ The pristine catalyst exhibited a BA site density that is comparable to our previously reported value (30 $\mu\text{mol}/\text{g}$).²⁰ Deposition of BHT (and an analogue, phenol) led to a four-fold decline in the peak areas of chemisorbed pyridine, which suggested ~25% of the original BA sites remained accessible. In the case of the I-3114 treated catalyst, no signs of protonated or strongly coordinated pyridine were measured in the spectrum (**Figure 4b**). Only bands at 1438 and 1596 cm^{-1} arose due to weakly bonded pyridine. This result indicated that BA sites were completely blocked by I-3114, which effectively shifted the MAB toward infinity and the activity to zero. On the contrary, ~25% of BA sites remained for BHT and I-1010, yielding finite, non-zero MAB and activity values.

The mechanism by which BA sites were depleted is related to the reaction of phenolic groups to form phenoxy species that were covalently bound to surface tungstate clusters. DRIFTS data for adsorbed phenol (**Figures S15, S16a**) confirmed the formation of phenoxy groups.

Hydrogenation of these phenoxy groups by Pt sites led to the formation of bound cyclohexanols, which subsequently desorbed or formed cyclohexene. Thus, some population of BA sites were regenerated and remained accessible to pyridine. BHT interaction with Pt/WO₃/ZrO₂ resembled that of phenol (**Figures S17, S16b**); however, the *t*-butyl groups of BHT effectively shielded the phenolic hydroxyl group from interaction with BA sites such that there was less catalyst poisoning at low temperatures. In this context, it is noteworthy that I-1010 exhibited more severe poisoning at high concentration, in comparison to pure BHT. This difference was likely due to the central ester groups in I-1010. During BA site-catalyzed hydrolysis,³⁰ surface carboxylate groups were more likely to form than phenoxy groups, which led to more severely blocked BA sites via steric effects (**Figure S16c**). For Pt catalysts, hydrogenation of aromatic rings in phenoxy species occurs at a higher rate than hydrogenation of carboxylates.³¹ Thus, it is expected that hindered phenolic antioxidants with non-hydrocarbon functional groups (*e.g.*, esters, amides) are likely to induce additional poisoning mechanisms and deactivate catalysts to greater degrees in comparison to BHT. An example of this effect was seen in the case of I-3114, which contained a central cyanuric acid group that was decomposed on Pt/WO₃/ZrO₂ at 250 °C as shown by a shift in the amidic carbonyl peak in the DRIFTS trace at increased temperatures (**Figure S18**). Furthermore, ~30% of phenolic hydroxyls did not interact with BA sites because of steric hindrance, which suggests that the combined effects of cyanuric acid derivatives contributed significantly to poisoning.

Overall, antioxidants induced complex changes to both metal and acid sites, which led to differences in activity and product selectivity. A schematic of the effects of the extremes of antioxidant-catalyst interaction (BHT vs. I-3114) is provided in **Figure 5**. The initial activity of the catalyst was largely determined by its MAB,²¹ the reaction conditions, and transport phenomena (discussed above). For the 1 wt% Pt and 25 wt% WO₃ on ZrO₂ catalyst used in this work, the native MAB (0.86 mol Pt/mol BA) promoted conversion of HDPE into light and mid-alkanes with moderate amounts of wax. In the presence of BHT, the catalyst lost significant activity because the number of total sites was reduced by blocking of metal sites or reaction with acid sites. The new effective MAB shifted product yields toward more mid-alkanes versus light alkanes, which equated to a general retardation in reaction kinetics. Higher exposure to poisonous additive caused by continuous throughput of plastic or lower catalyst loading likely would cause further damage, although regeneration via calcination in air could facilitate reuse of the catalyst. I-3114 blocked all Pt facet sites and leaves edge and corner sites intact, which yielded a catalyst with a similar number of metal sites as in the case of BHT poisoning; however, all BA sites were poisoned. Thus, the effective MAB increased towards infinity, and the activity was eliminated (because both metal and BA sites are required for hydrocracking). The resultant product consisted of only mid-alkanes, likely because transport of the antioxidant to the catalyst surface caused dynamic poisoning such that initial cracking products can accumulate to a small degree. Additionally, it should be expected that new antioxidant-derived chemical species can be generated during deconstruction because of the surface reactions of antioxidants with catalytic active sites, and these may lead to additional challenges to valorization processes (*e.g.*, further poisoning, product separations, reactor fouling). Due to the low concentration and strong catalyst binding affinity, no derivative species were identified in the present study.

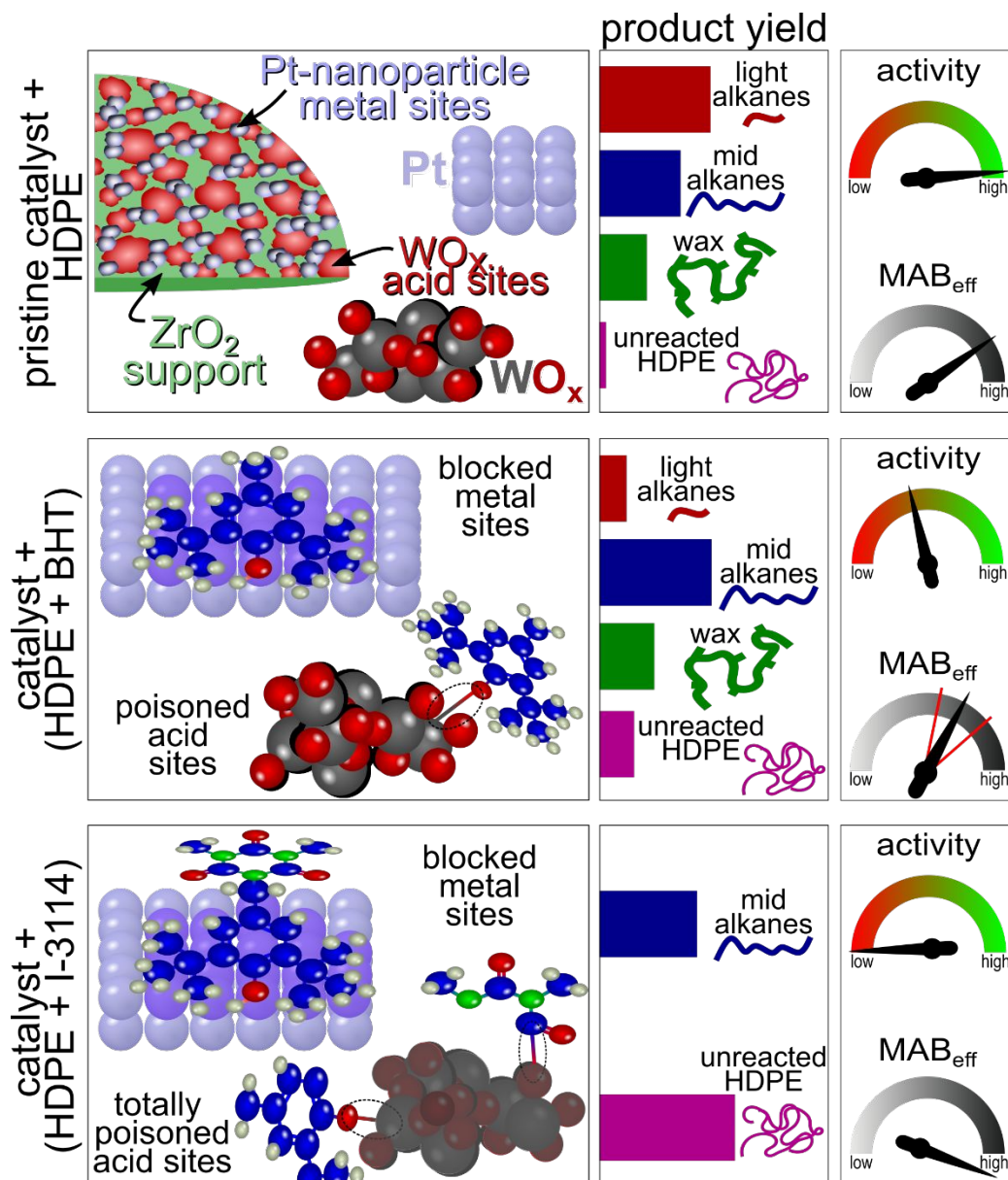


Figure 5. Schematic of the catalyst structure and antioxidant-induced catalyst transformations, relative product yields, and the approximate change to catalytic activity and effective metal-acid balance (MAB_{eff}). Activity is decreased in the presence of BHT and largely eliminated by I-3114. MAB_{eff} is slightly reduced by BHT (note the range, which depends on BHT concentration) and greatly increased by I-3114 (because the number of acid sites approaches zero, due to reaction with multiple I-3114 fragments). The product distribution is widely varied for the pristine catalyst, with little unreacted HDPE. For BHT-containing samples, mainly mid-alkanes and wax result, and for I-3114-containing specimens, mostly unreacted HDPE with modest amounts of mid-alkanes is recovered.

Conclusions

Additives are an intrinsic component of plastics, and therefore, plastics waste. In this work, we demonstrated the high activity of Pt/WO₃/ZrO₂ towards the deconstruction of HDPE. A comparison between as-received (*i.e.*, containing antioxidants and slip agents) HDPE and

stripped (*i.e.*, pure) HDPE revealed that the small-molecule additives present in the base HDPE formulations were responsible for a 50% reduction in catalyst activity. Additionally, the specific role of phenolic antioxidants on the reduction of extractable yield and alteration of product distribution was examined, as these additives are a major constituent of commercial plastics. Both antioxidant concentration and chemical structure had complex effects on the hydrocracking process. For BHT, an equilibrium adsorption concentration was reached, and concentration played a lesser role on reducing catalyst activity (*i.e.*, twofold in comparison to stripped HDPE). For I-1010, the presence of ester groups was the probable cause of a more dramatic decrease in activity and a stronger concentration dependence (*i.e.*, <2-fold and ~8-fold reductions at 0.5 wt% and 2 wt%, respectively). In the case of I-3114, nearly no conversion occurred as the cyanurate moieties appeared to lead to complete poisoning.

Using HT-GPC and DRIFTS analysis, we connected antioxidant-mediated transformations of our bi-functional catalyst to complex changes to hydrocracking-product distributions. Specifically, the phenolic groups of the antioxidant adsorbed to Pt metal sites and left only undercoordinated edges accessible to HDPE. Additionally, both phenolic groups and other moieties formed complexes with acid sites to change MAB and, therefore, selectivity toward certain product groups. For I-1010, ester groups were easily cleaved to form complexes with and reduce the number of acid sites, yielding a catalyst that was more selective toward mid-alkanes. The cyanurate group of I-3114 underwent additional reactions over Pt/WO₃/ZrO₂ to generate poisonous compounds that completely consumed acid sites that were required for activity. Based on these results, it may be desirable in some cases to pretreat plastics waste to remove certain additives that negatively affect catalytic deconstruction processes. Overall, there are substantial opportunities to either design additives that have lower impact on deconstruction outcomes or to develop robust valorization strategies that are agnostic to a range of real-world plastic additives.

Author contributions

Z. R. H., T. H. E., and L. T. J. K. conceived the idea. Z. R. H., P. A. K., M. S., and B. C. V. performed experiments and analysis. Z. R. H. and P. A. K. co-wrote the initial draft. D. G. V., T. H. E., and L. T. J. K. supervised the work and obtained funding. All authors contributed to the writing and editing of the manuscript.

Conflicts of interest

The authors declare no conflicts of interest.

Acknowledgements

This work was supported as part of the Center for Plastics Innovation, an Energy Frontier Research Center funded by the U.S. Department of Energy, Office of Science, Basic Energy Sciences, under award DE-SC0021166.

References

1. Z. R. Hinton, M. R. Talley, P. A. Kots, A. V. Le, T. Zhang, M. E. Mackay, A. M. Kunjapur, P. Bai, D. G. Vlachos, M. P. Watson, M. C. Berg, T. H. Epps, III and L. T. J. Korley, *Annual Review of Materials Research*, 2022, **52**, 249.
2. R. Geyer, J. R. Jambeck and K. L. Law, *Sci Adv*, 2017, **3**, e1700782.
3. T. H. Epps, III, L. T. J. Korley, T. Yan, K. L. Beers and T. M. Burt, *JACS Au*, 2022, **2**, 3.
4. L. T. J. Korley, T. H. Epps, III, B. A. Helms and A. J. Ryan, *Science*, 2021, **373**, 66.
5. J. N. Hahladakis and E. Iacovidou, *Sci Total Environ*, 2018, **630**, 1394.
6. J. N. Hahladakis, C. A. Velis, R. Weber, E. Iacovidou and P. Purnell, *J Hazard Mater*, 2018, **344**, 179.
7. J.-P. Lange, *ACS Sustainable Chemistry & Engineering*, 2021, **9**, 15722.
8. H. Wiesinger, Z. Wang and S. Hellweg, *Environ Sci Technol*, 2021, **55**, 9339.
9. *Polymer Modifiers and Additives*, CRC Press, Boca Raton, FL, 2018.
10. M. Tolinski, *Additives for Polyolefins: Getting the Most Out of Polypropylene, Polyethylene and TPO*, William Andrew, Waltham, MA, 2nd Ed. edn., 2015.
11. M. Bolgar, J. Hubball, J. Groeger and S. Meronek, *Handbook for the Chemical Analysis of Plastic and Polymer Additives*, CRC Press, Boca Raton, FL, 2008.
12. F. P. La Mantia, *Macromolecular Symposia*, 1998, **135**, 157.
13. *Recycling of Polymers: Methods, Characterization and Applications*, Wiley-VCH, Weinheim, Germany, 2017.
14. C. Ma, J. Yu, B. Wang, Z. Song, J. Xiang, S. Hu, S. Su and L. Sun, *Renewable and Sustainable Energy Reviews*, 2016, **61**, 433.
15. I. Vollmer, M. J. F. Jenks, M. C. P. Roelands, R. J. White, T. van Harmelen, P. de Wild, G. P. van der Laan, F. Meirer, J. T. F. Keurentjes and B. M. Weckhuysen, *Angew Chem Int Ed Engl*, 2020, **59**, 15402.
16. L. D. Ellis, N. A. Rorrer, K. P. Sullivan, M. Otto, J. E. McGeehan, Y. Román-Leshkov, N. Wierckx and G. T. Beckham, *Nature Catalysis*, 2021, **4**, 539.
17. G. W. Coates and Y. D. Y. L. Getzler, *Nature Reviews Materials*, 2020, **5**, 501.
18. P. A. Kots, B. C. Vance and D. G. Vlachos, *Reaction Chemistry & Engineering*, 2022, **7**, 41.
19. A. J. Martín, C. Mondelli, S. D. Jaydev and J. Pérez-Ramírez, *Chem*, 2021, **7**, 1487.
20. S. Liu, P. A. Kots, B. C. Vance, A. Danielson and D. G. Vlachos, *Sci Adv*, 2021, **7**, eabf8283.

21. B. C. Vance, P. A. Kots, C. Wang, Z. R. Hinton, C. M. Quinn, T. H. Epps, III, L. T. J. Korley and D. G. Vlachos, *Applied Catalysis B: Environmental*, 2021, **299**, 120483.
22. D. Munir, M. F. Irfan and M. R. Usman, *Renewable and Sustainable Energy Reviews*, 2018, **90**, 490.
23. E. G. Fuentes-Ordóñez, J. A. Salbidegoitia, M. P. González-Marcos and J. R. González-Velasco, *Industrial & Engineering Chemistry Research*, 2013, **52**, 14798.
24. J. W. Gosselink and W. H. J. Stork, *Industrial & Engineering Chemistry Research*, 1997, **36**, 3354.
25. BASF, *Irganox® 1010 Technical Information*, 2015, <https://dispersions-resins-products.basf.us/products/irganox-1010>, (accessed April 2022).
26. BASF, *Irganox® 3114 Technical Data Sheet*, 2019, https://documents.basf.com/7758655303a3460c5a14914b17d6cf15ffefc531/Irganox_3114_July_2019_R3_Adhesives.pdf, (accessed April 2022).
27. M. J. Kale and P. Christopher, *ACS Catalysis*, 2016, **6**, 5599.
28. Y. Yoon, R. Rousseau, R. S. Weber, D. Mei and J. A. Lercher, *J Am Chem Soc*, 2014, **136**, 10287.
29. T. Barzetti, E. Selli, D. Moscotti and L. Forni, *Journal of the Chemical Society, Faraday Transactions*, 1996, **92**, 1401.
30. Y. Wang, H. Ren, Y. Yan, S. He, S. Wu and Q. Zhao, *Polymers and Polymer Composites*, 2020, **29**, 1403.
31. M. Guo, X. Kong, C. Li and Q. Yang, *Communications Chemistry*, 2021, **4**, 54.